Electrochemical Design of Ultrathin Platinum-Coated Gold Nanoparticle Monolayer Films as a Novel Nanostructured Electrocatalyst for Oxygen Reduction

Yongdong Jin, Yan Shen, and Shaojun Dong*

State Key Laboratory of Electroanalytical Chemistry, Changchun Institute of Applied Chemistry, Chinese Academy of Sciences, Changchun 130022, Jilin, P.R. of China

Received: November 21, 2003; In Final Form: April 20, 2004

The deliberate tailoring of nanostructured metallic catalysts at the monolayer-level is an ongoing challenge and could lead to new electronic and catalytic properties, since surface-catalyzed reactions are extremely sensitive to the atomic-level details of the catalytic surface. In this article, we present a novel electrochemical strategy to nanoparticle-based catalyst design using the recently developed underpotential deposition (UPD) redox replacement technique. A single UPD Cu replacement with Pt^{2+} yielded a uniform Pt layer on colloid gold surfaces. The ultrathin (nominally monolayer-level) Pt coating of the novel nanostructured particles was confirmed by cyclic voltammetry and X-ray photoelectron spectra (XPS). The present results demonstrate that ultrathin Pt coating effects efficiently and behaves as the nanostructured monometallic Pt for electrocatalytic oxygen reduction, and also shows size-dependent, tunable electrocatalytic ability. The as-prepared ultrathin Pt-coated Au nanoparticle monolayer electrodes reduce O_2 predominantly by four electrons to H_2O, as confirmed by the rotating ring-disk electrode (RRDE) technique.

Introduction

Electrocatalytic reactions are of central important in electrochemistry and play a vital role in emerging technologies related to environmental and energy-related applications, such as fuel cells. The large surface-to-volume ratios and size-dependent catalytic properties of fine particles in homogeneous and heterogeneous catalysis constitute part of the driving force in developing nanoparticle catalysts.[1,2] Three types of catalytic nanoparticles are of recent interest: 1) nanoparticles supported on metals, oxides, or polymers,[1,3−5] 2) nanoparticles encapsulated in dendrimers,[6] and 3) nanoparticles encapsulated in alkanethiolate monolayers.[7] Among them, late transition metals are of great significance in chemical catalysis.[8] For example, Pt-group nanoparticles in the size range of 2−10 nm, employed commercially in fuel cells and related applications, exhibit interesting variations in electronic[9] and coordinative[10] properties.

Since surface-catalyzed reactions are extremely sensitive to the atomic-level details of the catalytic surface,[11] the deliberate tailoring of the nanostructured catalysts is an ongoing challenge and could lead to new electronic and catalytic properties. However, examples of catalyst design on the basis of fundamental, surface science-based insight are extremely few.[2,12−13] Recent successful examples, for example, include the design of a gold−nickel surface alloy catalyst for stream reforming,[12] the controlled electrodeposition of Pd on Au(111) with well-defined surface composition to study directly the role of atomic ensembles in the reactivity of bimetallic electrocatalysts,[13] the preparation of small metal nanoclusters via an STM tip and for their catalytic efficiency studies,[14] and the tailoring of monolayer-encapsulated metallic nanoparticles as catalysts for electrocatalytic oxidation of carbon monoxide and methanol stems.[2] Although Pt submonolayers on Ru nanoparticles have been exploited as a high CO tolerance fuel cell electrocatalyst,[15] to the best of our knowledge electrochemical modification of ultrathin (even monolayer-level) Pt overlayers on a gold nanoparticle surface has not yet been exploited for catalytic applications to date.

Recently, Weaver et. al.[16] perfected the underpotential deposition (UPD) redox replacement technique[17] to prepare an Au nanoparticle film electrode modified with uniform Pt-group overlayers (down to 1−2 monolayers) and succeeded in surface-enhanced Raman scattering (SERs) applications. In this article, we adapt the UPD-replacement tactics to design Pt overlayer-coated Au nanoparticle monolayer films and extend for electrocatalytic applications. The present results demonstrate that the ultrathin Pt coating effects efficiently and behaves as the nanostructured monometallic Pt for electrocatalytic oxygen reduction and shows core size-dependent, tunable electrocatalytic ability. A single UPD Cu replacement with Pt^{2+} yielded a uniform Pt overlayer, as indicated by pinhole-free characteristics using voltammetric characterizations. The ultrathin Pt coating of the novel nanostructured particle nature was also confirmed by X-ray photoelectron spectra (XPS). The as-prepared ultrathin Pt-coated Au nanoparticle monolayer electrodes reduce O_2 predominantly by four electrons to H_2O, as confirmed by the rotating ring-disk electrode (RRDE) technique. The findings are important and may provide an interesting way to effectively prepare Pt catalysts that efficiently use this expensive metal.

Experimental Section

Chemicals. All aqueous solutions were made with deionized water, which was further purified with a Milli-Q system (Millipore). The following materials were obtained from Aldrich: $HAuCl_4 \cdot 3H_2O$, trisodium citrate dihydrate, (3-aminopropyl)trimethoxysilane (APTMS), $NaBH_4$, K_2PtCl_4, 4-ammonobenzoic acid (4-ABA), and poly(diallyldimethyl) ammonium chloride (PDDA). HCl, HNO_3, $HClO_4$, H_2SO_4, $CuSO_4$, and indium tin oxide (ITO) electrodes were obtained from China. All chemicals, unless mentioned otherwise, were of analytical grade and were used as received.

* Corresponding author: (e-mail) dongsj@ns.ciac.jl.cn.

10.1021/jp0375517 CCC: $27.50
Published on Web 05/20/2004

Synthesis of Gold Colloids. The 3 ± 1 nm and 20 ± 2 nm gold colloids used in this study were prepared as described in detail elsewhere.[18,19] All glassware used in the following procedures were cleaned in a bath of freshly prepared 3:1 HCl: HNO_3 (aqua regia) and rinsed thoroughly in H_2O prior to use. Preparation of Au "seed colloid" solution of ca. 3 ± 1 nm-diameter particles was preceeded by adding 1 mL of 1% aqueous $HAuCl_4 \cdot 3H_2O$ to 100 mL of H_2O with vigorous stirring, followed by the addition of 1 mL of 1% aqueous sodium citrate one min later. After an additional one minute, 1 mL of 0.075% $NaBH_4$ in 1% sodium citrate was added. The solution was stirred for 5 min and then stored at 4 °C until needed.[18] The 20 ± 2 nm gold colloids were prepared, according to Frens,[19] by heating a 50 mL solution of 0.01% $HAuCl_4$ to boiling and adding 0.75 mL of 1% sodium citrate, then maintaining boiling for 10 min and cooling. (The solutions are stored at 4 °C.) The average particle diameters were characterized by transmission electron microscopy (TEM).

Preparation of Ultrathin Pt−Coated Gold Nanoparticle Monolayer Films. The preparation procedures of ultrathin platinum-coated gold nanoparticle monolayer films are as follows: First, a carefully cleaned indium tin oxide (ITO) electrode was modified by immersion into a solution of 3-aminopropyltrimethoxysilane (APTMS) in methanol for 12 h, yielding amine-terminated surface-functionalities for gold nanoparticle assembling.[20] Then, the gold nanoparticles were immobilized onto the APTMS-modified ITO surface by immersion of the latter into the solution for more than 12 h. A UPD monolayer of copper was formed on the nanoparticle monolayer film by holding the potential at 0 V in 0.1 M H_2SO_4 containing 1 mM $CuSO_4$, then transferred to a solution of 5 mM K_2PtCl_4 in deaerated 0.1 M $HClO_4$. The electrode was left in this solution at an open circuit for 10 min to ensure complete redox replacement of the UPD Cu, then rinsed and immersed in the voltammetric cell for electrochemical experiments.

Electrochemistry. Cyclic voltammetry was performed with a CHI 660 electro-chemical workstation (USA) in a conventional three-electrode electrochemical cell using colloids-modified ITO as the working electrode, twisted platinum wire as the auxiliary electrode, and KCl-saturated Ag/AgCl as the reference electrode. Electrochemical measurements were all recorded and reported versus the KCl-saturated Ag/AgCl reference electrode. Solutions were purged with highly purified nitrogen for at least 20 min prior to a series of experiments. An EG&G PARC Model 366 bi-potentiostat was used for rotating ring-disk voltammetry experiments. A rotating glassy carbon (GC) disk-platinum ring electrode was used as a working-electrode. The collection efficiency (N) of the ring electrode obtained by reducing ferricyanide at a disk electrode was 0.139. The GC electrode was first derivative with 4-amonobenzoic acid (4-ABA) according to the published procedures[21] and the subsequent poly(diallyldimethyl) ammonium chloride (PDDA, 8% aqueous solution) electrostatic assembly for 40 min. The PDDA modified electrode was then used to prepare nanostructured monolayer films using the above-mentioned same procedures. For RRDE experiments performed in air-saturated 0.1 M H_2SO_4, disk potential was scanned from +0.50 to −0.20 V while ring potential was kept at +1.0 V in order to detect any H_2O_2 evolved at the disk.

Instrumentation. Samples for TEM were prepared by placing a drop of solution onto a carbon-coated copper grid and were examined by using a JEOL 2010 transmission electron microscopy operated at 200 kV. Analysis of the X-ray photoelectron spectra (XPS) was performed on an ESCLAB MKII using Mg as the exciting source.

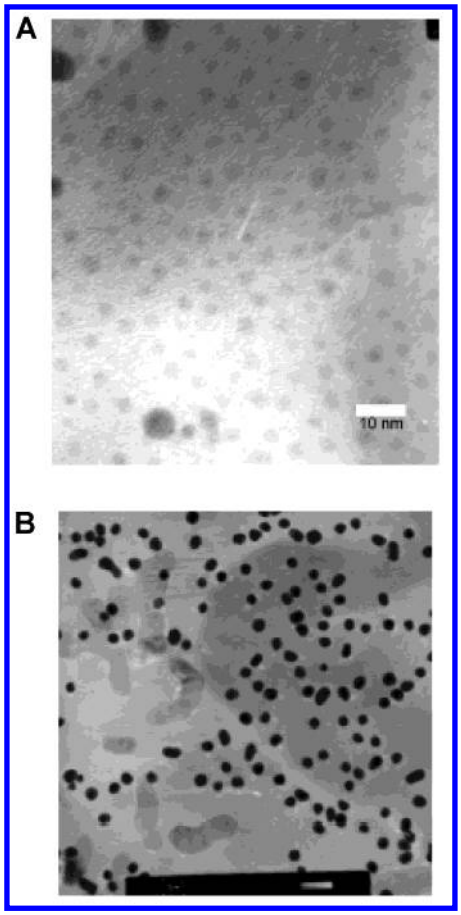

Figure 1. TEM images of gold nanoparticles used: (A) 3 ± 1 nm (scale bar = 10 nm), (B) 20 ± 2 nm (scale bar = 50 nm) in diameter.

Results and Discussion

Electrochemical Design and Characterizations of Ultrathin Platinum-Coated Gold Nanoparticle Monolayer Films. The attractiveness of gold nanoparticles as templates for catalyst design includes the ability to prepare routinely monodispersed colloidal nanoparticles having a wide diameter range (1.5 to 100 nm), along with the availability of surface chemistry, such as self-assembly ability. To examine the influence of gold sizes on the electrocatalytic activity for oxygen reduction, we use here two Au nanoparticle templates (3 ± 1 nm and 20 ± 2 nm in diameter, respectively) to prepare ultrathin platinum-coated gold nanoparticle catalysts. The 3 ± 1 nm gold colloids were prepared as described by Natan et. al.[18a] and Jin et. al.[18b] The 20 ± 2 nm gold colloids were prepared according to Frens.[19] The average particle diameters were characterized by transmission electron microscopy (TEM), as shown in Figure 1.

The cleaned indium tin oxide (ITO) electrodes were modified by immersion into a solution of 3-aminopropyltrimethoxysilane (APTMS) in methanol, yielding amine-terminated surface-functionalities, as described by Jin et al.,[20] for gold nanoparticle assembling. Then the gold nanoparticles were immobilized onto the APTMS-modified ITO surface by immersion of the latter into the solution for more than 12 h. The colloid coating appears as a continuous red-violet film. The Au colloid film is stable and is not washed off from the ITO surface upon repeated rinsing with water. The typical colloid film on the amine-terminated ITO surface is ∼20−30% of close-packing coverage. The less-than-complete monolayer coverage results from the finite size of particles and from interparticle repulsion.[22] The typical coverages are $\sim 8 \times 10^{11}$ particles/cm^2 and $\sim 4 \times 10^{10}$ particles/cm^2, for 3 ± 1 nm and 20 ± 2 nm gold colloids,

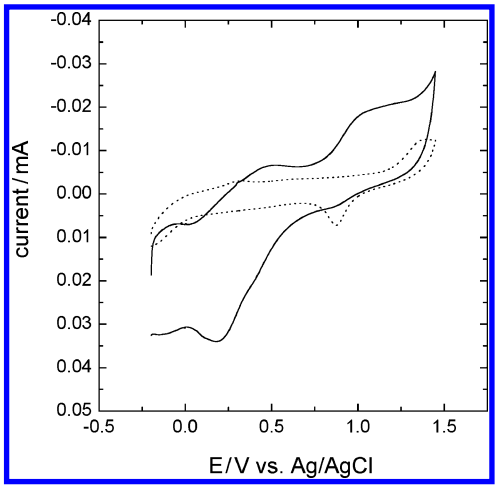

Figure 2. Cyclic voltammograms (50 mV S^{1-}) for 3 ± 1 nm gold nanoparticle films on APTMS-modified ITO substrates in 0.1 M H_2SO_4 before (dotted trace) and after (solid trace) coating with monolayer-level Pt. Electrode area, ~0.4 cm^2.

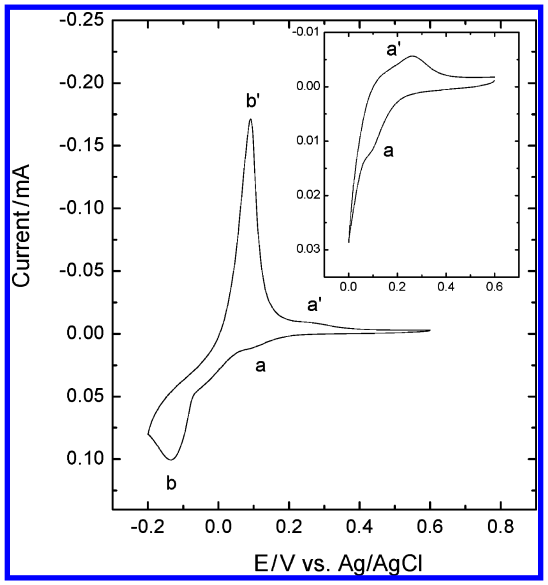

Figure 3. Cyclic voltammograms (20 mV S^{1-}) for a 3 ± 1 nm gold nanoparticle film electrode in 1 mM $CuSO_4$ + 0.1 M H_2SO_4. Electrode area, ~0.4 cm^2. Inset shows the UPD part of the cyclic voltammogram.

respectively, as well characterized by Natan[18a] and Willner.[23] Figure 2 (dotted trace) shows a representative cyclic voltammogram (CV) obtained (at 50 mV s^{-1}) from − 0.20 to 1.45 V versus a KCl-saturated Ag/AgCl electrode at the resulted 3 ± 1 nm gold nanoparticle monolayer-modified electrode in 0.1 M H_2SO_4. The presence of a wide "double-layer" region below circa 0.7 V and the anodic formation and cathodic removal of oxide at higher potentials are familiar features of gold electrochemistry. The large current in the "double-layer" region might be a reflection of the nanoparticle nature of the electrode surface.[16]

A UPD copper monolayer was deposited thereafter. Figure 3 shows a representative CV (20 mV s^{-1}) for a 3 ± 1 nm gold nanoparticle monolayer-modified electrode in a deaerated 1 mM $CuSO_4$ + 0.1 M H_2SO_4 solution. On the negative-going sweep, two main cathodic features (a and b) are observed at ca. + 0.1 and − 0.1 V, respectively. Feature a is consistent with the formation of UPD copper,[24] while feature b refers to bulk copper deposition. As expected, two anodic peaks (b′ and a′) are obtained on the positive-going sweep, corresponding to dissolution of bulk and UPD copper, respectively. Although the sweep rates (both at 20 mV s^{-1}) are the same, the Cu UPD peaks are poorly visible as compared to that of the roughened bulk gold electrode reported by Mrozek et al.[25] Since the CV profile of Cu UPD is similar to Figure 3 for the 20 ± 2 nm particle film electrode, the discrepancy may stem from the high surface nanoparticles nature of the film electrode, which causes solute depletion at this relatively high sweep rate. Also, unlike UPD on a bulk gold electrode, there is considerable current at 0.0 V (as shown in Figure 3) that does not appear to be due simply to underpotential deposition. Underpotential deposition is not the only source of current, otherwise current should decay to zero once a monolayer or two of Pt is deposited. The considerable current at 0.0 V is found to be nanoparticle size-dependent and would arise from the addition of the electrocatalytic current of fine gold nanoparticles because we found that the smaller the gold nanoparticles, the larger the current at 0.0 V. Knowing the density of the Au colloids (~8×10^{11}/cm^2) and their average size (~2.6 nm in diameter), along with the Cu UPD charge (~3.5 μC), stemmed from the CV and the geometric electrode area (~0.4 cm^2), one can estimate the average number of Cu atoms deposited on each Au nanoparticle. In the case of ~2.6 nm colloid Au, the average number was calculated to be ~30, indicative of the submonolayer nature of the Cu coatings. To ensure full completion of nearly monolayer Cu deposition, a UPD monolayer of Cu was formed by holding the potential for ~5−10 s at 0 V in 0.1 M H_2SO_4 containing 1 mM $CuSO_4$. It is also noteworthy to mention that the potentials of the features are mediated by nanoparticles and are size-dependent.[25]

The solid trace in Figure 2 is the corresponding cyclic voltammogram obtained after the deposition of an ultrathin Pt coating, using the procedure described by Park et. al.,[16] as follows. First, a UPD monolayer of copper was formed on the gold nanoparticle monolayer film by holding the potential at 0 V in 0.1 M H_2SO_4 containing 1 mM $CuSO_4$, then transferred to a solution of 5 mM K_2PtCl_4 in deaerated 0.1 M $HClO_4$. The electrode was left in this solution at an open circuit for 10 min. The period of time was chosen to ensure complete redox replacement of UPD Cu and ordering of the resultant Pt overlayer.[25] The electrode was then rinsed and immersed in the voltammetric cell. The spontaneous 1:1 Cu/Pt replacement procedure, yielding an epitaxial Pt overlayer, is driven by the difference between equilibrium potentials for the Pt and the UPD Cu redox couples.[16,25] The preparation procedure is schematically illustrated in Scheme 1. Significantly, the resulting CV provides clear evidence that the Au nanoparticle surface is modified by the platinum. The anodic−cathodic current profile, comprised of near-reversible weak peaks associated with hydrogen desorption-adsorption and irreversible features corresponding to the formation and removal of surface oxide, are characteristic of a nanoparticulated Pt surface and is consistent with the reported profile.[16,25] In particular, the presence of the platinum oxide reduction peak at ca. 0.2 V, along with the near-absence of the corresponding gold oxide feature at circa 0.85 V, shows that few exposed Au sites (<10%) remain. After several CV cycles, the weak peak at 0.85 V is almost invisible, indicating the essentially "pinhole-free" nature of the ultrathin (monolayer-level) Pt coating.[16] The uniformity of such Pt overlayers on a gold nanoparticle surface formed with Pt^{2+} is indeed confirmed previously by surface-enhanced Raman scattering (SERs), employing carbon monoxide as a "probe" chemisobate.[16,25] Incidentally, the asymmetry of the anodic−cathodic current profile, comprised of near-reversible peaks associated with hydrogen desorption-adsorption, does not

SCHEME 1: Schematic Illustrations of Preparation Procedures of Ultrathin (nominally monolayer-level) Platinum-coated Gold Nanoparticle Monolayer Films on an ITO Electrode Surface

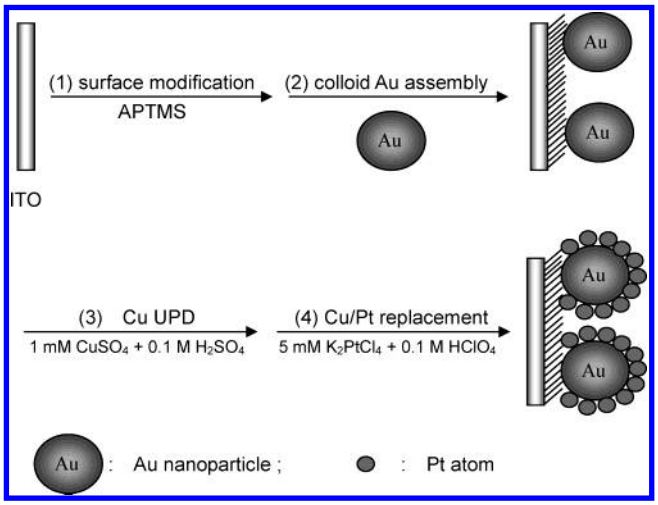

originate from the surface contamination of the nanostructured catalysts because the current profile is similar and reproducible even after we deliberately cleaned the surfaces by adsorbing CO and a subsequent stripping treatment. Although the exact origins are not clear yet and need further investigations, the asymmetry of the current profile would arise from the addition of an electrocatalytic current of oxygen reduction caused by traces of oxygen, and would be indicative of high electrocatalytic efficiency of the fine nanostructured bimetal catalysts in 0.1 M H_2SO_4, although the cyclic voltammogram was recorded immediately after the solution was purged with highly purified nitrogen for ~20 min.

The as-prepared Pt-coated gold nanoparticles are in principle an ultrathin (down to 1−2 monolayers) Pt coating[16] since we started with a UPD Cu monolayer and followed with a 1:1 spontaneous redox replacement reaction of surface-confined UPD Cu with Pt^{2+}

($Cu_{UPD} + Pt^{2+} \rightarrow Cu^{2+} + Pt$). The chemical nature of the ultrathin Pt-coated gold nanoparticles was further confirmed by X-ray photoelectron spectra (XPS). XPS after the Cu UPD shows a small Cu $2P_{3/2}$ peak at 932.2 eV (Figure 4A, curve 1). The small peak above the noise level is indicative of the ultrathin nature of the UPD Cu shells. After the 1:1 redox replacement reaction with Pt^{2+}, the colloid surfaces are Cu-free, as shown in curve 2. The monometallic colloid Au (2~4 nm) $4f_{7/2}$ peak shifts from 82.9 to 83.2 eV upon deposition of ultrathin Pt (Figure 4B, curves 1 and 2) due to the interactions of foreign Pt atoms with colloidal Au, which may influence the electronegative potential of metal through the inherent surface plasmons (SPs) interaction of the colloid metal films. Meanwhile, some damping of intensity occurs. A small Pt 4f peak at ~72.5 eV (Figure 4C, curve 1) after the 1:1 Cu/Pt redox replacement reaction is indicative of the ultrathin nature of the Pt coating. The Au and Pt content of the colloid monolayer films is roughly estimated by Au 4f and Pt 4f peak areas and an average composition of ~6:1 (Au:Pt) is given. As the average thickness of the colloid Au (2~4 nm) monolayer films is within the X-ray penetration depth (~3 nm), the Pt coating is ultrathin and quantitatively down to 1−2 monolayers. The XPS data are poor (small signal) due to the low Au coverage (~20−30% of close-packing coverage) and the monolayer-level Cu or Pt deposition. The XPS data are credible (not just random noise) because similar spectra were seen for three parallel samples. It is

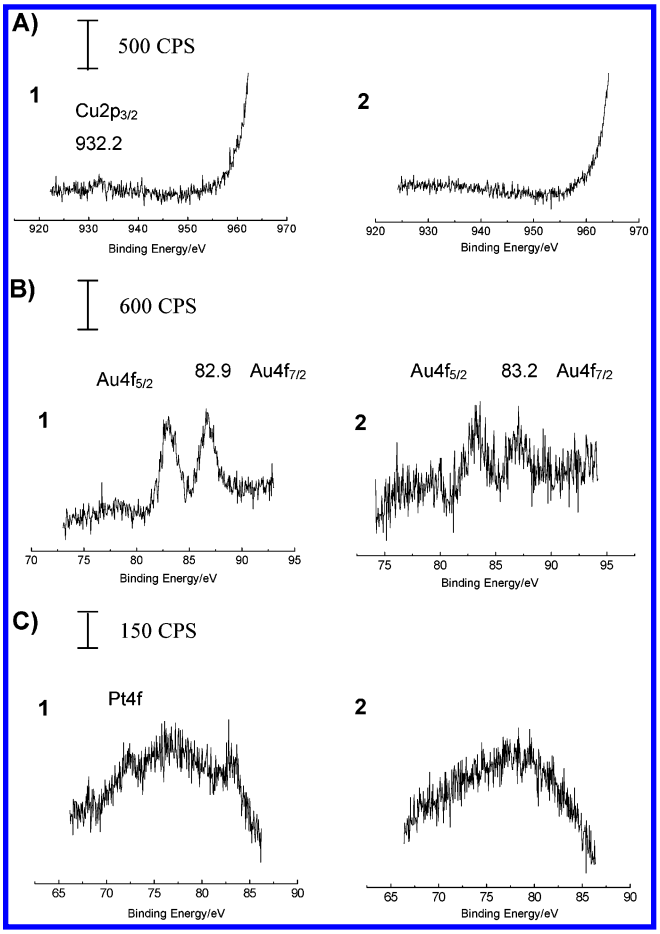

Figure 4. XPS spectra of ITO/APTMS/colloid Au (2~4 nm) monolayers shows (A) Cu 2p: after Cu UPD (curve 1) and Cu/Pt redox replacement (curve 2); (B) Au 4f: before (curve 1) and after ultrathin Pt deposition (curve 2); (C) Pt 4f: after ultrathin Pt deposition (curve 1). Curve 2 is a control spectrum obtained on an ITO/APTMS electrode (Au-free) after the same preparations.

noteworthy to mention that the ultrathin Pt deposits only on the colloid Au surface, *not* on the ITO surface. In control experiments (Pt does deposit in the absence of Au or UPD Cu), the absence of Pt was confirmed by XPS analysis, as shown in Figure 4C, curve 2. Unambiguously, the XPS analysis combined with the electrochemical characterizations prove the chemical nature of the ultrathin Pt-coated gold nanoparticle monolayer films.

Although the as-designed nanostructures are nominally of Au/Pt core−shell structure, the XPS data alone are not convincing for the claim about the novel Au/Pt core−shell structure. In fact, the XPS data could be just due to the presence of very little Pt on the colloid gold surface in any form, and a homogeneous surface alloy involving the same relative number of Pt and Au atoms would have, in all likelihood, given the same spectrum. Also, it is impossible to conclude that Pt has not agglomerated to form tiny clusters leaving parts of areas of basal Au exposed to the solution. However, CV of the nanostructured electrode in 0.1 M H_2SO_4 shows that few exposed Au sites remain during the successive cycling and the uniformity and essentially "pinhole-free" nature of the ultrathin Pt coating,[16] which exclude from the possibility of surface alloying and severe agglomeration and suggest strongly the essentially core−shell type of the nanostructure.

Electrocatalysis of Oxygen Reduction. Of central interest here are the electrocatalytic behaviors of the as-prepared ultrathin Pt-covered bimetallic nanoparticle films. To assess the

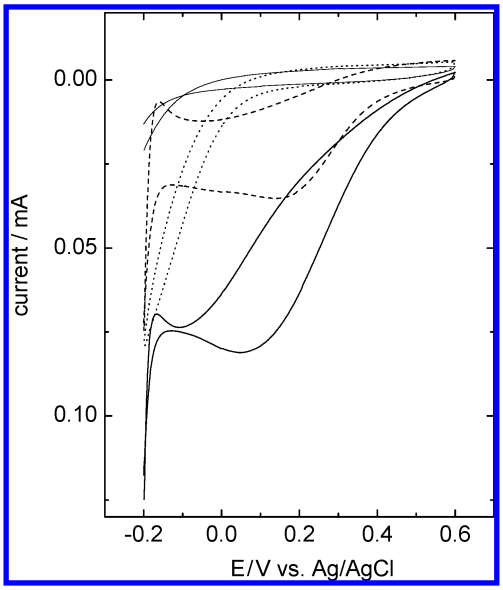

Figure 5. Cyclic voltammograms at bare 3 ± 1 nm gold nanoparticle film (dotted trace), ultrathin Pt-covered 3 ± 1 nm gold nanoparticle film (dashed trace), and bare (solid trace, top) and corresponding ultrathin Pt-covered 20 ± 2 nm gold nanoparticle film (solid trace, bottom) electrodes in O_2-saturated 1.0 M H_2SO_4. The scan rate was 50 mV S^{1-}. Electrode area, ~0.4 cm^2.

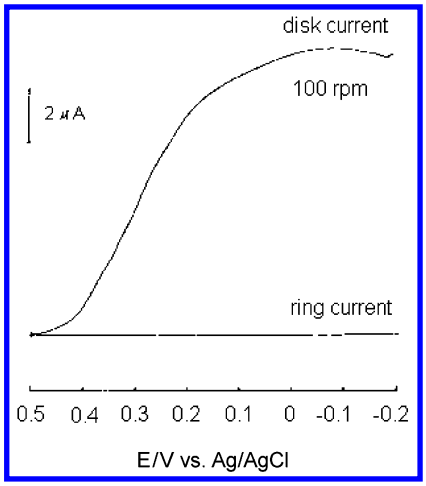

Figure 6. Current-potential curves for the reduction of air-saturated O_2 at a rotating platinum ring-graphite disk electrode with ultrathin Pt-coated Au nanoparticles monolayer adsorbed on the disk electrode. The potential of the ring electrode was maintained at 1.0 V. Rotation rate: 100 rpm. Scan rate: 50 mV S^{1-}. The supporting electrolyte was 0.1 M H_2SO_4.

influence of the ultrathin (nominally monolayer-level) Pt coating on the electrocatalytic behaviors and to verify the core size-dependent, tunable electrocatalytic activity (dictated by the size of the gold nanoparticles used), we examined the electrocatalytic oxygen reduction of the system. The solid trace (top) and the solid trace (bottom) in Figure 5 show CVs at bare and ultrathin Pt-covered 20 ± 2 nm gold nanoparticle monolayer films in oxygen-saturated 1.0 M H_2SO_4. Oxygen reduction begins at ~0.5 V (vs Ag/AgCl) and the reduction peak centered at ~0.1 V for the ultrathin Pt-covered 20 ± 2 nm gold nanoparticle monolayer films, while little reduction current appears for corresponding bare gold nanoparticle monolayer films from +0.6 to −0.1 V. The reduction potential (solid trace, bottom) is more positive than those reported by Dai and Bruening[26] or Crooks and Zhao[6b] for reduction-formed Pt nanoparticles in multilayered polyelectrolyte films[26] and dendrimer-encapsulated Pt nanoparticles.[27] The results provide clear evidence that the electrocatalytic oxygen reduction behaviors of gold nanoparticles are effected efficiently and even behave as the nanostructured monometallic Pt even though only ultrathin (down to 1−2 monolayers) Pt coatings are present. This point is grateful to design catalysts for practical application since it is possible to save precious metal, such as Pt, by optimizing the synthetic conditions so that only very thin surface layers occur.

The core size-dependent, tunable electrocatalytic ability of oxygen reduction is examined by using two nanoparticle templates, that is, 3 ± 1 nm (Figure 1A) and 20 ± 2 nm (Figure 1B), respectively. With the 3 ± 1 nm gold nanoparticle instead of the 20 ± 2 nm ones, the bare 3 ± 1 nm Au nanoparticle films show little reduction current from +0.6 to +0.1 V. Oxygen reduction begins at ~ +0.1 V, as shown in Figure 5 (dotted trace, top). The ultrathin Pt-covered 3 ± 1 nm Au nanoparticle monolayer films show more catalytic activity, in that the overpotential for oxygen of the resulting nanostuctured electrode was decreased by ca. 100 mV (comparing the dashed trace to the solid trace (bottom) in Figure 5). Both catalytic films are almost fully electroactive and the current for oxygen reduction of the two specimens is a function of the "real" area of the electrode, that is, the sum of the electrochemically accessible areas of the individual particles, as confirmed by the concordance of the experimental current ratio of the two specimens with the calculated ratio $(i_{3\pm1}/i_{20\pm2} \propto (r^2d)_{3\pm1}/(r^2d)_{20\pm2} = (1.5^2 \times 8 \times 10^{11})/(10^2 \times 4 \times 10^{10}) = 0.45)$. The stability of the as-prepared nanoparticle film electrodes was tested by successive potential cycling in O_2-saturated 1.0 M H_2SO_4 solution at ambient temperature. No detectable peak shift was observed after ~1 h of successive potential cycling, indicative of the absence of severe sintering of the immobilized monolayer nanoparticles during the process.

The as-prepared ultrathin Pt-coated Au nanoparticle monolayer electrodes reduce O_2 predominantly by four electrons to H_2O, as confirmed by the rotating ring-disk electrode (RRDE) technique. Figure 6 shows voltammetric curves of the ultrathin Pt-coated Au (2~4 nm) nanoparticle monolayers recorded with the use of an RRDE electrode for O_2 reduction in aqueous 0.1 M H_2SO_4. In these experiments, disk potential was scanned from +0.50 to −0.20 V while ring potential was kept at +1.0 V in order to detect any H_2O_2 evolved at the disk. A large disk current was obtained whereas almost no ring current was observed (even when ring current is enlarged 10 times, not shown here), suggesting that the as-prepared nanostructured electrocatalysts reduce O_2 predominantly by four electrons to H_2O. The collection efficiency (N) of the ring electrode obtained by reducing ferricyanide at the disk electrode was 0.139. From the ratio of the ring-disk current, the electron-transfer number (n) of 3.98 is calculated according to the equation $n = 4 - 2(I_R/I_DN)$.[27]

Conclusions

In conclusion, we present here a novel electrochemical strategy to nanoparticle-based catalyst design using the UPD redox replacement technique. The preliminary results demonstrate that ultrathin (nominally monolayer-level) Pt coating effects efficiently and behaves as novel nanostructured Pt for electrocatalytic reduction of oxygen to water and shows core size-dependent, tunable electrocatalytic ability. A single UPD Cu replacement with Pt^{2+} yielded an ultrathin and uniform Pt layer on colloid gold surfaces. The ultrathin (down to 1−2 monolayers) Pt coating and the essentially Au/Pt core−shell type of the nanostructured particle films were confirmed by X-ray photoelectron spectra (XPS) combined with electrochemi-

cal characterizations. The as-prepared nanoparticle monolayer electrodes reduce O_2 predominantly by four electrons to H_2O, as confirmed by the rotating ring-disk electrode (RRDE) technique.

The advantages of the method are obvious. First, it grateful to design catalysts for practical application since it is possible to save precious metal, like Pt, only by surface modification of another cheaper metal. Second, given that UPD provides a straightforward method to modify metal surfaces with an ordered, epitaxial metal overlayer with a variety of metals (such as Ag, Pd, Cu, Hg, etc.), along with the nanoparticle-based core−shell tuning in terms of core composition, size, shape, and surface properties, the reported strategy could prove to be universal for a variety of metals and will be attractive for use in the design of nanoparticle-based materials for catalytic applications, especially in fuel cells and in sensors, because UPD-modified surfaces show increased resistance to poisoning from oxidation products.[28]

Acknowledgment. This work was supported by the National Natural Science Foundation of China (No. 20075028; 20211130506).

References and Notes

(1) Valden, M.; Lai, X.; Goodman, D. W. *Science* **1998**, *281*, 1647.
(2) Zhong, C.-J.; Maye, M. M. *Adv. Mater.* **2001**, *13*, 1507.
(3) (a) Friedrich, K. A.; Henglein, F.; Stimming, U.; Unkauf, W. *Electrochim. Acta* **2000**, *45*, 3283. (b) Heemeier, M.; Carlsson, A. F.; Naschitzki, M.; Schmal, M.; Bäumer, M.; Freund, H.-J. *Angew. Chem. Int. Ed.* **2002**, *41*, 4073. (c) Biswas, P. C.; Nodasaka, Y.; Enyo, M.; Haruta, M. *J. Electroanal. Chem.* **1995**, *381*, 167.
(4) Bond, G. C.; Thompson, D. T. *Catal. Rev.* **1999**, *41*, 319.
(5) Hepel, M. *J. Electrochem. Soc.* **1998**, *145*, 124.
(6) (a) Crooks, R. M.; Zhao, M.; Sun, L.; Chechik, V.; Yeung, L. K. *Acc. Chem. Res.* **2001**, *34*, 181. (b) Zhao, M. Q.; Crooks, R. M. *Adv. Mater.* **1999**, *11*, 217. (c) Scott, R. W. J.; Datye, A. K.; Crooks, R. M. *J. Am. Chem. Soc.* **2003**, *125*, 3708.
(7) (a) Maye, M. M.; Lou, Y.; Zhong, C. J. *Langmuir* **2000**, *16*, 7520. (b) Lou, Y.; Maye, M. M.; Han, L.; Luo, J.; Zhong, C. J. *Chem. Commun.* **2001**, 473. (c) Luo, J.; Jones, V. W.; Maye, M. M.; Han, L.; Kariuki, N. N.; Zhong, C.-J. *J. Am. Chem. Soc.* **2002**, *124*, 13988.
(8) For an overview, see: Aiken, J. D.; Finke, R. G. *J. Mol. Catal. A* **1999**, *145*, 1.
(9) Tong, Y.; Rice, C.; Wieckowski, A.; Oldfield, E. *J. Am. Chem. Soc.* **2000**, *122*, 1123.
(10) Park, S.; Wasileski, S. A.; Weaver, M. J. *J. Phys. Chem. B* **2001**, *105*, 9719.
(11) Somorjai, A. G. *Introduction to surface chemistry and catalysis*; Wiley: New York, 1994.
(12) Besenbacher, F.; Chorkendorff, I.; Clausen, B. S.; Hammer, B.; Molenbroek, A. M.; Nørskov, J. K.; Stensgaard, I. *Science* **1998**, *279*, 1913.
(13) Maroun, F.; Ozanam, F.; Magnussen, O. M.; Behm, R. J. *Science* **2001**, *293*, 1811.
(14) (a) Kolb, D. M.; Ullmann, R.; Will, T. *Science* **1997**, *275*, 1097. (b) Kolb, D. M.; Ullmann, R.; Ziegler, J. C. *Electrochim. Acta* **1998**, *43*, 2751. (c) Meier, J.; Friedrich, K. A.; Stimming, U. *Faraday Discuss.* **2002**, *121*, 365. (d) Del, P. M.; Leiva, E.; Kleine, H.; Meier, J.; Stimming, U.; Mariscal, M.; Schmickler, W. *Appl. Phys. Lett.* **2002**, *81*, 2635.
(15) Brankovic, S. R.; Wang, J. X.; Adzic, R. R. *Electrochem. Solid ST.* **2001**, *4*, A217.
(16) Park, S.; Yang, P. X.; Corredor, P.; Weaver, M. J. *J. Am. Chem. Soc.* **2002**, *124*, 2428.
(17) Brankovic, S.; Wang, J. X.; Adzić, R. R. *Surf. Sci.* **2001**, *474*, L173.
(18) (a) Grabar, K. C.; Allison, K. J.; Baker, B. E.; Bright, R. M.; Brown, K. R.; Freeman, R. G.; Fox, A. P.; Keating, C. D.; Musick, M. D.; Natan, M J. *Langmuir* **1996**, *12*, 2353. (b) Jin, Y. D.; Kang, X. F.; Song, Y. H.; Zhang, B. L.; Cheng, G. J.; Dong, S. J. *Anal. Chem.* **2001**, *73*, 2843.
(19) Frens, G. *Nature Phys. Sci.* **1973**, *241*, 20.
(20) Jin, Y. D.; Dong, S. J. *Chem. Commun.* **2002**, 1780.
(21) Liu, J.; Cheng, L.; Liu, B.; Dong, S. *Langmuir* **2000**, *16*, 7471.
(22) Grabar, K. C.; Smith, P. C.; Davis, J. A.; Musick, M. D.; Jackson, M. A.; Walter, D. G.; Guthrie, A. P.; Natan, M. J. *J. Am. Chem. Soc.* **1996**, *118*, 1148.
(23) Doron, A.; Katz, E.; Willner, I. *Langmuir* **1995**, *11*, 1313.
(24) Kolb, D. M. In *Advances in Electrochemistry and Electrochemical Engineering*; Gerischer, H., Tobias, C. W., Eds.; Wiley: New York, 1978; vol. 11, p 125.
(25) Mrozek, M. F.; Xie, Y.; Weaver, M. J. *Anal. Chem.* **2001**, *73*, 5953.
(26) Dai, J. H.; Bruening, M. L. *Nano Lett.* **2002**, *2*, 497.
(27) Liu, S.; Xu, J.; Ran, H.; Li, D. *Inorg. Chim. Acta* **2000**, *306*, 87.
(28) Manne, S.; Hansma, P. K.; Massie, J.; Elings, V. B.; Gewirth, A. A. *Science* **1991**, *251*, 183 and references therein.